PCIM Europe 2019; International Exhibition and Conference for Power Electronics, Intelligent Motion, Renewable Energy and Energy Management; Proceedings of

Benchmark Study on Impedance Identification Methods for Grid Connected Converters

M. Petkovic and D. Dujic

POWER ELECTRONICS LABORATORY
ÉCOLE POLYTECHNIQUE FÉDÉRALE DE LAUSANNE

Benchmark Study on Impedance Identification Methods for Grid Connected Converters

Marko Petković, Dražen Dujić

Power Electronics Laboratory, École Polytechnique Fédérale de Lausanne (EPFL), Switzerland

Corresponding author: Marko Petković, marko.petkovic@epfl.ch

Abstract

The increasing number of renewable energy sources connected to the grid also introduces large number of different power electronics converters into the system. This paper provides a comparative benchmark of methods to identify the frequency characteristics of a grid connected converter model. Analytical open-loop and closed-loop models are verified through offline simulations and real-time hardware-in-the-loop measurements. To verify the model and identify the transfer functions linking input and output variables, a pseudo-random binary sequence signal is used for perturbation in both cases.

1 Introduction

The combination of the increasing energy demand, the trend of increased environmental awareness and the recent advances in the field of power electronics have made possible for the renewable energy systems to become an important part of the energy generation today. The integration of renewable energy sources and power conversion efficiency to the power system is made possible due to utilization of grid connected converters and as such, they are becoming an important part of modern energy systems [1]. As an example, battery storage systems make use of power converter to convert the ac power into the dc power as well as the increasing number of electric charging stations for electric vehicles. Amongst others, this conversion is made possible by a single or three-phase active rectifiers, an Active Front End (AFE) (see Fig. 1). As modern energy systems are becoming power electronics dominated, new interactions between power electronics equipment and the power systems are starting to take place. The issues related to power electronics equipment are harmonic instabilities and degradation of power quality level [2]–[4]. To combat these problems, there exists a need to characterize the Power Electronics (PE) converter before it is integrated in a power system.

Modelling a PE converter requires a systematic approach from an early stage of the development. The first step in the design process is the verification of open-loop model. Even though the open-loop model is the simplest one and a converter would not be used as such in practice, in order to characterize more complex systems one would have to confirm the open-loop model and build up on it. In practice, the only useful and realistic way of operating the converter is in the closed-loop. A closed-loop model includes dynamic effects of different control and synchronization loops. Making their influence evident stems directly from the open-loop model. In order to be able to confirm all the design steps a PE engineer needs to know all the characteristics of the system being designed. Before the prototyping phase, a verification of various system components is needed. One of the means of assuring this is to use Hardware-in-the-Loop (HIL) tools. HIL techniques have been increasingly used to aid the development and verification of power electronics systems [5], [6]. Such methods are attractive as they offer possibilities to simulate the system in real-time under various operating conditions and investigate the influence of modifying different system parameters such as the parameters of the control or synchronization loops. HIL simulation environment enables rapid prototyping of converter control and power stages, or even capturing the effect of interfacing it to other systems as is the case in renewable energy systems. Authors of [7] have demonstrated how larger HIL

ISBN 978-3-8007-4938-6

systems can be effectively used to characterize output impedance of an inverter with LC output filter. This work aims to further demonstrate the feasibility and applicability of HIL tools to the verification of the input characteristics of AFE converter

2 Active Front End

Small-signal models of the AFE, presented in Fig. 1, have been first developed in [8] and recently detailed in [9]. All of the modelling presented is done in the *dq*-frame. In a voltage-fed AFE system, considered here for the reasons of simplicity, input variables are the dc-voltage v_{dc}, grid voltages $v_{\mathrm{g,d}}$ and $v_{\mathrm{g,q}}$ and the converter duty cycles $d_{\mathrm{c,d}}$ and $d_{\mathrm{c,q}}$. The output variables are the DC current i_{dc} and output currents $i_{\mathrm{g,d}}$ and $i_{\mathrm{g,q}}$. The easiest way of representing the AFE open-loop input-output dynamics is through a matrix assembling all transfer functions that relate different inputs to their respective outputs. Such a matrix is given with:

$$\begin{bmatrix} \mathbf{i}_{\mathrm{dc}} \\ \mathbf{i}_g \end{bmatrix} = \begin{bmatrix} \mathbf{Y}_{\mathrm{out,o}} & \mathbf{T}_{\mathrm{oi,o}} & \mathbf{G}_{\mathrm{ci,o}} \\ \mathbf{G}_{\mathrm{io,o}} & -\mathbf{Y}_{\mathrm{in,o}} & \mathbf{G}_{\mathrm{co,o}} \end{bmatrix} \begin{bmatrix} \mathbf{v}_{\mathrm{dc}} \\ \mathbf{v}_g \\ \mathbf{d}_c \end{bmatrix} \quad (1)$$

Where the subscript "o" denotes it is an open-loop characteristics. Different transfer functions relating inputs and outputs in Eq. (1) are:

- $\mathbf{Y}_{\mathrm{out,o}}$ - output admittance matrix
- $\mathbf{T}_{\mathrm{oi,o}}$ - input-to-output reverse transfer function matrix
- $\mathbf{G}_{\mathrm{ci,o}}$ - control-to-input transfer function matrix
- $\mathbf{G}_{\mathrm{io,o}}$ - forward transfer function matrix
- $\mathbf{Y}_{\mathrm{in,o}}$ - input admittance matrix
- $\mathbf{G}_{\mathrm{co,o}}$ - control-to-output transfer function matrix

Each of these transfer functions show how the change within an input variable influences an output one. The transfer functions are easily obtainable either analytically by solving state-space equations presented in [9] or in a simulation, as well as in a real system, by perturbing an input variable and measuring the result it has on the output. The open-loop model of the AFE directly depends on its operating point. Depending on the operating point, it is impractical to verify the model in a real system, since a small perturbation of an input variable might give considerably large response

Tab. 1: Model parameters

$P_{\mathrm{in}} = 67\mathrm{kW}$	$v_{\mathrm{dc}} = 1.2\mathrm{kV}$
$v_{\mathrm{g,d}} = 580\mathrm{V}$	$f_g = 50\mathrm{Hz}$
$v_{\mathrm{g,q}} = 0\mathrm{V}$	$L_{\mathrm{AFE}} = 1.8\mathrm{mH}$
$i_{\mathrm{g,d}} = 55\mathrm{A}$	$R_{\mathrm{AFE}} = 10\mathrm{m\Omega}$
$i_{\mathrm{g,q}} = 0\mathrm{A}$	$f_{\mathrm{sw}} = 10\mathrm{kHz}$

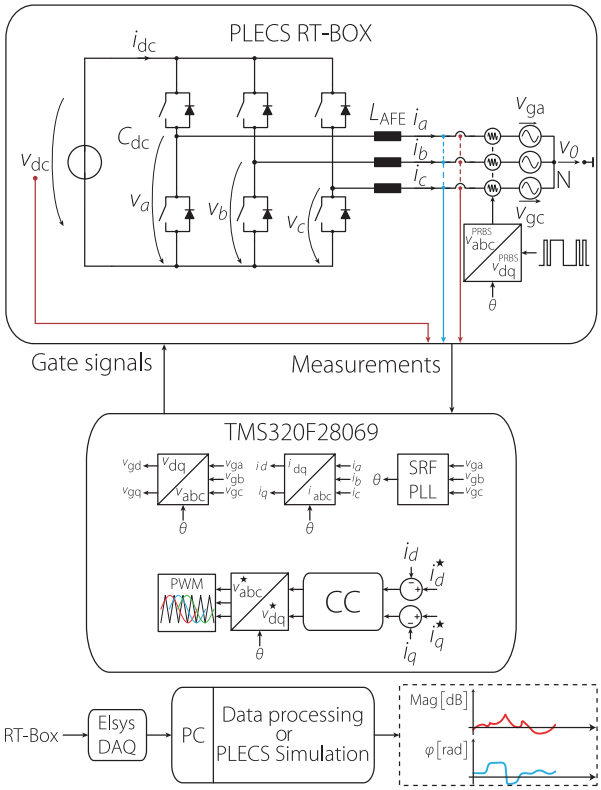

Fig. 1: Grid connected voltage-fed active front end.

of an output variable. On the other side, since the voltage source in a real system is not ideal, it affects the model. To mimic the real system as close as possible, the best approach is to use HIL simulations. This work relies on the HIL system, RT-Box realized by Plexim, implemented in order to verify transfer functions obtained analytically and in an offline PLECS simulation. In this particular case, the AFE presented is a part of a larger system intended to be employed as a grid emulator and a perturbation injection converter for impedance measurement [10], [11] and as a such the operating point of the AFE is set to its full power operating point. Parameters of the system are presented in Tab. 1.

ISBN 978-3-8007-4938-6

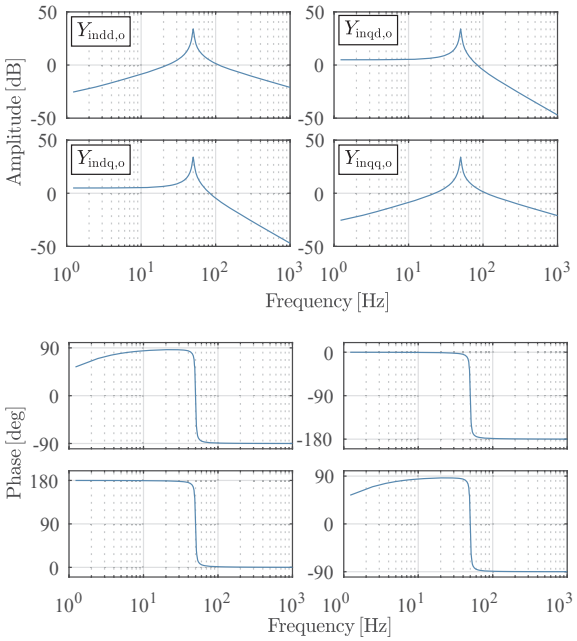

Fig. 2: Open-loop $\mathbf{Y}_{\mathrm{in,o}}$ input admittance magnitude and phase

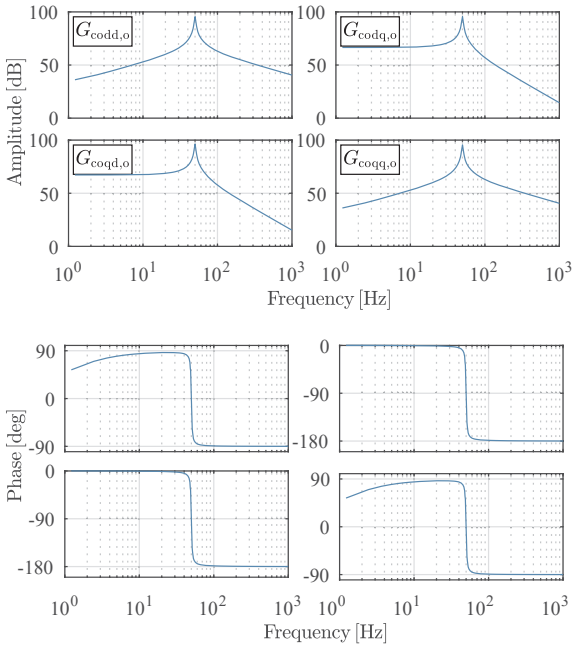

Fig. 3: $G_{\mathrm{codd,o}}$ control-to-output magnitude and phase

In the beginning stages of the design process, the most important characteristics of the model are the open- and closed-loop input admittance, $\mathbf{Y}_{\mathrm{in,o}}$ and $\mathbf{Y}_{\mathrm{in,cl}}$, which can be obtained through the same approach. More complicated models that include dynamic behaviour of control and grid synchronization loop are just an extension of the most basic transfer functions. Figs. 2 to 5 show $Y_{\mathrm{in,o}}$, $G_{\mathrm{co,o}}$, $Y_{\mathrm{in,cl}}$ and G_{cc} characteristics obtained analytically.

Extending on the AFE open-loop characteristics, closed-loop admittance shows the influence of including the feedback control in the model. Once the current control loop is closed, the *d*-axis input admittance is given as:

$$Y_{\mathrm{indd,cl}} = \frac{Y_{\mathrm{indd,o}}}{1+G_{\mathrm{cc}}} \tag{2}$$

Where G_{cc} is the current control open-loop gain and is given by:

$$G_{\mathrm{cc}} = H_d G_{\mathrm{ci}} G_{\mathrm{codd,o}} G_{\mathrm{PWM}} \tag{3}$$

Where H_d, G_{ci}, $G_{\mathrm{codd,o}}$ and G_{PWM} are the current sensor, current controller, open-loop control-to-output and modulator transfer functions, respectively. It is obvious that modifying the switching frequency, sampling time or control parameters shows the influence on the closed-loop input admittance and can be effectively used to avoid instability issues related to input admittance / output impedance interactions.

3 Offline vs. Real-Time simulations

Analytical models can easily be verified through offline simulations, though for a large number of simulations and operating points this kind of approach is tedious and sub-optimal. As opposed to offline simulations, real-time ones can be used to speed up the process thanks to RT-HIL tools. Applying these tools facilitates the fast verification of the design and reveals the influence of modifications to the design. For this application, HIL method using RT-Box, presented in Fig. 1, was used to perform the real-time simulation of an open-loop and closed-loop voltage-fed AFE. The angle needed for the transformation was generated directly in the RT-Box. In order to attain the best precision and avoid numerical errors due to discretization, the model time step in RT-Box has to be set as low as possible. For this application the discretization time step was set to $t_d = 5\,\mu\mathrm{s}$. RT-Box together with the Elsys TraNET 408s data acquisition (DAQ) instrument is presented in Fig. 9.

ISBN 978-3-8007-4938-6

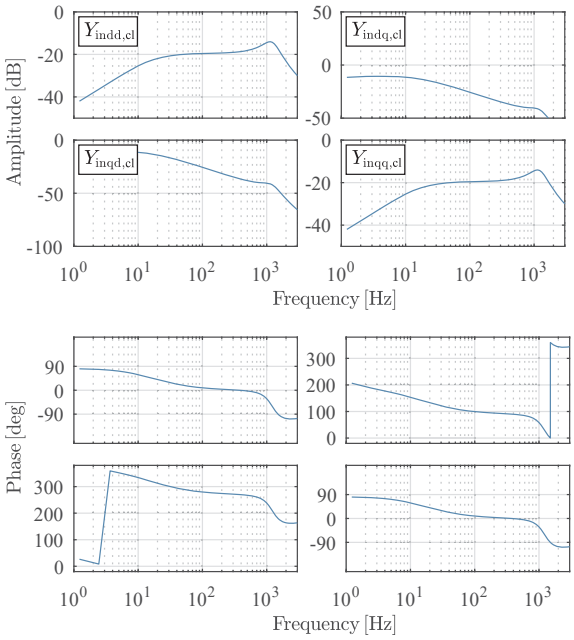

Fig. 4: Closed-loop $\mathbf{Y}_{\mathrm{in,cl}}$ input admittance magnitude and phase

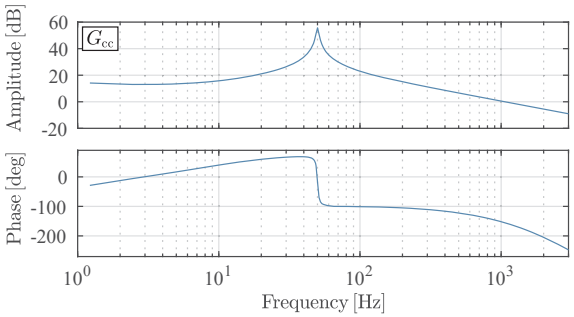

Fig. 5: Gain loop G_{cc} magnitude and phase

3.1 Control

The control algorithm is implemented in the TMS320F28069M Digital Signal Processor (DSP). Grid voltage and grid current are measured and provided to PLECS RT-Box analog outputs that are directly interfaced to the DSP ADC channels. Measurements are sampled at $f_s = 10\mathrm{kHz}$. This implementation allows for straightforward adjustment of control parameters. Using the ePWM peripheral module present in the DSP, gate pulse signals are sent to the RT-Box where real-time HIL model runs.

The grid angle θ for the transformations is generated in the PLECS model, while the angle for control purposes is obtained by the Phase-Locked-Loop (PLL) implemented in the DSP. The control algorithm implemented is the decoupled Syncronous Reference Frame (SRF) current controller. The current control is performed at a rate of 10 kHz. To obtain gate signals, Sinusoidal Pulse-Width-Modulation (SPWM) at 10 kHz is used.

Tab. 2: Current control parameters

$k_{\mathrm{p,i}} = 11.8$	$k_{\mathrm{i,i}} = 0.12$	$\phi_{\mathrm{m,i}} = 36.5°$

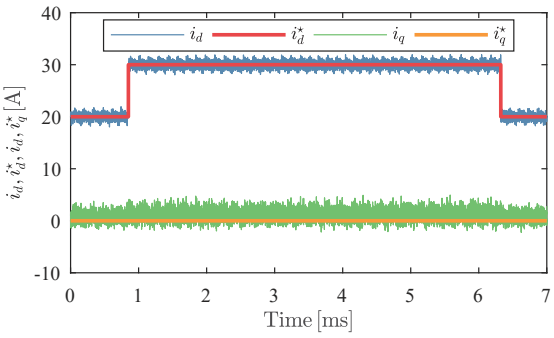

Fig. 6: Current controller response to step change of $i_d^\star$

The controller is optimally tuned to obtain the desired response to step reference change. Controller parameters are summarized in Tab. 2. Current control loop performance to reference step change is presented in Fig. 6.

3.2 PRBS signal for perturbation

Type of signals used for perturbation is the Pseudo-Random Binary Sequence (PRBS) signal. This type of signals is well-know and was successfully used for similar applications [12], [13]. The advantage of such a signal is its frequency content. As it is a wideband signals, its energy stays constant over a wide range and then falls to zero at its generation frequency. This makes the measurement faster than if a narrowband signals was used, such as a sinusoidal sweep. The PRBS signal can easily be created using feedback shift register circuits. In RT-Box model implementation this is equivalent to using signal delays (see Fig. 7). Creating such a signals in the control system of a converter is a straightforward task and is a preferred method when creating a perturbation internally [14]. There exist numerous subtypes of PRBS signals but for this application the Maximum-Length Binary Sequence (MLBS) is used [15]. The

ISBN 978-3-8007-4938-6

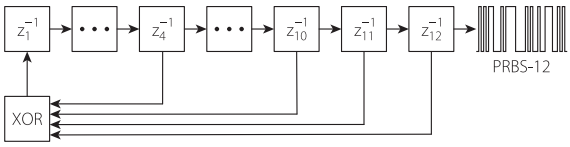

Fig. 7: Shift register circuit for PRBS generation

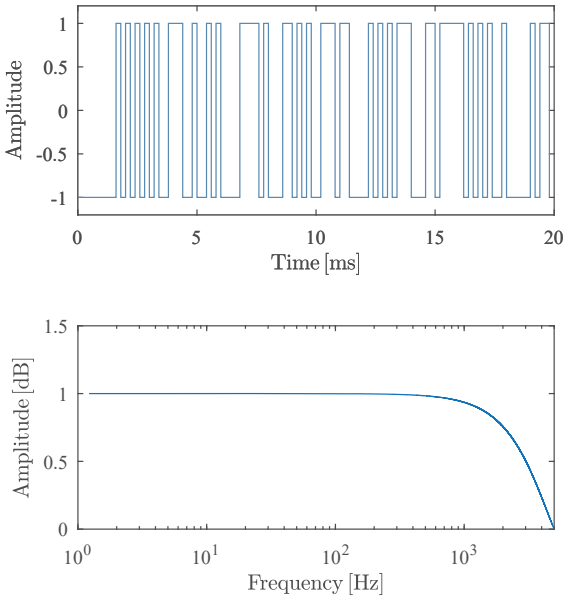

Fig. 8: PRBS-12 signal in time and frequency domain

MLBS is a periodic signal satisfying the relation:

$$a_k = \sum_{i=1}^{n} c_i a_{k-i} \tag{4}$$

and with a sequence length $N = 2^n - 1$, where n is the number of bits in the sequence. For this particular application the PRBS-12 signals is used with a 4095-bit-length MLBS. The sequence is created at 5 kHz, which gives a frequency resolution of 1.221 Hz. The PRBS-12 signal in time and frequency domain is presented in Fig. 8. For the brevity issues, only a part of the time domain signal is presented.

3.3 Data collection

In order to collect measurements for processing and impedance calculation, the DAQ instrument Elsys TraNET 408s with its proprietary TranAX 3 DAQ software is used [16], [17]. Measurements are gathered directly from RT-Box analog output and sampled at a sampling rate of 80 kHz. Measurements are gathered in block size of 128 kS which sets the measurement time at 1.638 s, i.e. two PRBS-12 cycles are measured. Collected measurements are exported for processing which is done using MATLAB.

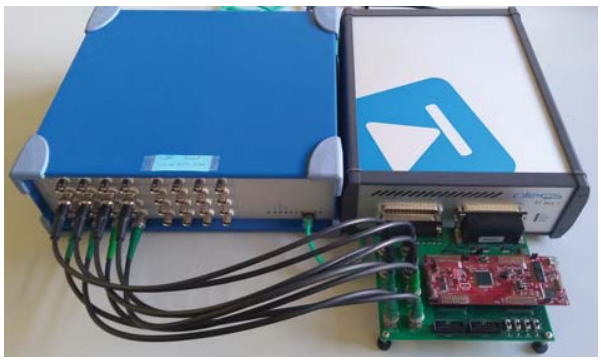

Fig. 9: PLECS RT-Box and Elsys TraNET 408s DAQ instrument.

3.4 Offline simulations

All of the previously presented elements have been implemented in a similar way in the offline simulations in PLECS software. Control and perturbation methods are common to both types of simulations while the data collection is performed directly inside the software. Using the offline simulations avoids the imprecisions and delays due to the Analog-to-Digital Conversion (ADC) and communication chain between the RT-Box and the DSP. However, these effects are unavoidable in a real system and their absence in an offline simulation provokes a loss of information.

4 Benchmark Results

The open-loop and closed-loop impedance $\mathbf{Y}_{\mathrm{in,o}}$ and $\mathbf{Y}_{\mathrm{in,cl}}$ are extracted after performing the FFT on the measurements and obtaining their frequency domain characteristics. In the frequency domain, omitting (f) operator for brevity, $\mathbf{Y}_{\mathrm{in,o}}$ and $\mathbf{Y}_{\mathrm{in,cl}}$ are given as:

$$\mathbf{Y}_{\mathrm{in}} = \begin{bmatrix} Y_{\mathrm{indd}} & Y_{\mathrm{indq}} \\ Y_{\mathrm{inqd}} & Y_{\mathrm{inqq}} \end{bmatrix} \tag{5}$$

To confirm the HIL methods presented, admittance obtained analytically is compared against the same admittance which is a result of offline simulation inside PLECS software and real-time simulation

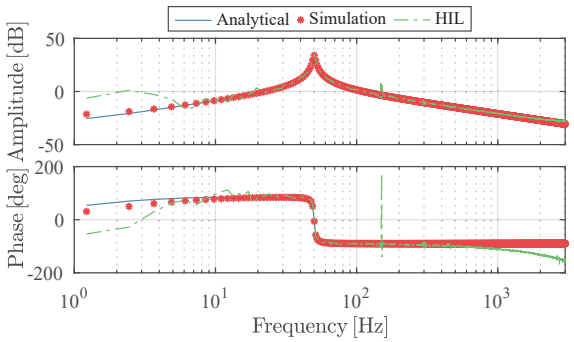

Fig. 10: $Y_{\mathrm{indd,o}}$ open-loop input admittance magnitude and phase

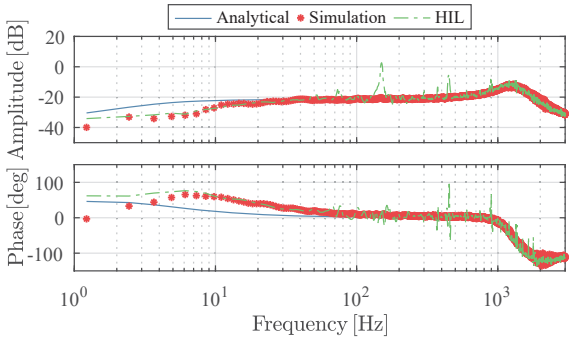

Fig. 11: $Y_{\mathrm{indd,cl}}$ closed-loop input admittance magnitude and phase

inside RT-Box. All the results are presented up to the frequency of 3 kHz as it is considered that up to that frequency the PRBS signals have a satisfactory energy. Open-loop admittance in *d*-axis is presented in Fig. 2. It is noticeable that the analytical model is confirmed with offline and real-time simulation over the majority of the frequency range.

The impact of closing the current control loop is shown through the closed-loop input admittance presented in Fig. 11. It is visible that the methods presented once again show a good match between the analytical models and its offline and real-time simulation counterparts. Moreover, the real-time simulations can better make obvious the harmonics presents. The differences between the analytical model and real-time simulations are mostly related to the ADC issues and processing of measurements inside the DSP.

5 Conclusion

Assessment of various transfer functions, particularly of input admittance (impedance) of closed-loop controlled power electronics converters, provide valuable information, indicating dynamic behaviour in relevant environment. As presented in the paper, RT-HIL tools provide efficient and fast way to carry out investigations beyond analytical predictions and faster than with use of offline simulations. While the relatively simple example is presented, usefulness of these methods is already recognised in the power electronics community. Nevertheless, care has to be taken during implementation in order to avoid numerical troubles due to RT-HIL tools themselves.

References

[1] R. Teodorescu, M. Liserre, and P. Rodriguez, *Grid converters for photovoltaic and wind power systems*. John Wiley & Sons, 2011, vol. 29.

[2] X. Wang and F. Blaabjerg, “Harmonic stability in power electronic based power systems: Concept, modeling, and analysis”, *IEEE Transactions on Smart Grid*, pp. 1–1, 2018.

[3] T. Messo, J. Jokipii, A. Aapro, and T. Suntio, “Time and frequency-domain evidence on power quality issues caused by grid-connected three-phase photovoltaic inverters”, in *2014 16th European Conference on Power Electronics and Applications*, 2014, pp. 1–9.

[4] U. Javaid, F. D. Freijedo, D. Dujic, and W. van der Merwe, “Dynamic assessment of source–load interactions in marine mvdc distribution”, *IEEE Transactions on Industrial Electronics*, vol. 64, no. 6, pp. 4372–4381, 2017.

[5] H. Seo, M. Park, I. Yu, and B. Song, “Performance analysis and evaluation of a multifunctional grid-connected pv system using power hardware-in-the-loop simulation”, in *2011 Twenty-Sixth Annual IEEE Applied Power Electronics Conference and Exposition (APEC)*, 2011, pp. 1945–1948.

[6] F. D. Freijedo, E. Rodriguez-Diaz, and D. Dujic, “Stable and passive high-power dual active bridge converters interfacing mvdc grids”,

IEEE Transactions on Industrial Electronics, vol. 65, no. 12, pp. 9561–9570, 2018.

[7] P. Jonke, M. Makoschitz, B. Sumanta, J. Stoeckl, and H. Ertl, "Ac-sweep analysis and verification of an ac power source with virtual output impedance for validation of grid connected components", in *PCIM Europe 2017; International Exhibition and Conference for Power Electronics, Intelligent Motion, Renewable Energy and Energy Management*, 2017, pp. 1–7.

[8] S. Hiti, D. Boroyevich, and C. Cuadros, "Small-signal modeling and control of three-phase pwm converters", in *Proceedings of 1994 IEEE Industry Applications Society Annual Meeting*, vol. 2, 1994, 1143–1150 vol.2.

[9] T. Suntio, T. Messo, and J. Puukko, *Power electronic converters: dynamics and control in conventional and renewable energy applications*. John Wiley & Sons, 2017.

[10] N. Hildebrandt, M. Petković, and D. Dujić, "Evaluation of 1.7 kV SiC MOSFETs for a regenerative cascaded H-bridge multilevel converter cell", in *2018 IEEE International Conference on Industrial Technology (ICIT)*, 2018, pp. 718–723.

[11] N. H. M. Petković and D. Dujić, "Medium voltage impedance-admittance measurement system based on the cascaded h-bridge multilevel converter", *Electronics*, vol. 32, no. 2, pp. 829–841, 2019.

[12] R. Luhtala, T. Roinila, and T. Messo, "Implementation of real-time impedance-based stability assessment of grid-connected systems using mimo-identification techniques", *IEEE Transactions on Industry Applications*, vol. 54, no. 5, pp. 5054–5063, 2018.

[13] T. Messo, A. Aapro, and T. Suntio, "Generalized multivariable small-signal model of three-phase grid-connected inverter in dq-domain", in *2015 IEEE 16th Workshop on Control and Modeling for Power Electronics (COMPEL)*, 2015, pp. 1–8.

[14] T. Roinila, T. Messo, R. Luhtala, R. Scharrenberg, E. de Jong, *et al.*, "Hardware-in-the-loop methods for real-time frequency-response measurements of on-board power distribution systems", *IEEE Transactions on Industrial Electronics*, pp. 1–1, 2018.

[15] K. Godfrey, *Perturbation signals for system identification*. Prentice Hall International (UK) Ltd., 1993.

[16] E. AG, *Tranet fe data acquisition instrument datasheet*, 2016.

[17] ——, *Tranax 3 data acquisition application software user manual*, Aug. 28, 2014.

ISBN 978-3-8007-4938-6